REGIONAL INTRARENAL PERFUSION IN MAN: AN ASSESSMENT WITH THE SCINTILLATION CAMERA

M. Kinoshita, B. L. Holman, R. E Zimmerman, D. F. Adams, S. J. Adelstein, and N. K. Hollenberg

Harvard Medical School and Peter Bent Brigham Hospital, Boston, Massachusetts

The importance of intrarenal perfusion patterns in a number of physiologic and pathophysiologic states has led to increasing interest in radioxenon for assessing this parameter in man. In this study the scintillation camera has been used to evaluate concentric and segmental xenon turnover in normal man and in patients with hypertension and acute oliguric renal failure. In healthy kidneys the area of the image defined by the isotope decreased approximately 20% in the first minute after injection, a finding compatible with a cortical flow rate greater than that in the remainder of the kidney. Intrarenal flow rates defined with the camera were identical to those measured with a probe-mounted detector; however, recirculation did contribute to probe-recorded tail components.

In patients with oliguric renal failure, the study confirmed the absence of a rapid flow component. Failure of the size of the renal image to decrease, as it does normally, strongly supports the hypothesis of a preferential reduction in cortical perfusion. Washout of isotope from the superior and inferior renal poles was relatively homogeneous in normal man; however, there were quantitatively significant differences in segmental washout in patients with nephrosclerosis or chronic pyelonephritis.

These studies provide strong support for current concepts of normal renal perfusion in which the rapid component of xenon washout represents cortical perfusion; they also confirm a model of acute renal failure in which there is a preferential reduction in cortical perfusion; and they suggest the presence of segmental renal perfusion abnormalities in patients with essential hypertension.

A number of methods applied to assessment of intrarenal blood flow in animals have revealed striking differences in the perfusion of various anatomic zones within the kidney (*1–9*). Outer cortical blood flow rates are extremely high in all species studied and with all methods utilized. Progressively lower flow rates have been found in the inner cortex, outer medulla, and papilla.

Of the methods used to assess intrarenal perfusion in animal models, the inert gas washout method has found the widest application in man (*2,9*). Autoradiography has localized the tracer's compartmental distribution in the dog kidney (*2,9*). The most rapid and largest component represents cortical perfusion. In man, strikingly similar washout is observed but only indirect evidence provides anatomic localization. Correlations with function, gross and microscopic morphology, and the renal arteriogram first suggested that the rapid component in man also represents cortical perfusion (*9–16*). Recently the scintillation camera has provided more direct support for this contention although it is not conclusive (*17,18*). The kidney image produced with xenon decreased in size during washout implying more rapid disappearance from the cortex. The instrumentation utilized, however, provided an ambiguous result because image size on the oscilloscope screen is sensitive not only to the dimensions of the object but also to the incident count density. Because the activity in the kidney decreased with time, an apparent reduction in the size of the kidney image could have occurred without a more rapid

Received Nov. 6, 1973; revision accepted April 8, 1974.

For reprints contact: Norman K. Hollenberg, Dept. of Radiology, Peter Bent Brigham Hospital, 721 Huntington Ave., Boston, Mass. 02115.

disappearance of isotope from the renal cortex. In the present study, additional instrumentation used in conjunction with the Anger scintillation camera has been used to provide a more rigorous test of the hypothesis and to assess segmental renal perfusion in man.

METHODS

Subjects. Ten normal potential kidney donors and 14 patients with hypertension were studied at the time of selective renal arteriography. Hypertensive patients were categorized as having "essential" hypertension, renovascular hypertension, and chronic pyelonephritis according to standard diagnostic criteria (*19*). One of the patients with chronic pyelonephritis also had primary aldosteronism. Five studies were performed in four additional patients who had acute oliguric renal failure secondary to shock, prolonged ischemia, acute vasculitis, or allograft rejection.

Techniques. The techniques used for selective renal artery catheterization and administration of radioxenon have been described (*10–14*). A number of modifications were made for this protocol. The xenon dose was 10–20 mCi in 1–2 ml of saline. The patient's expired breath was vented with an air pump into a hood to prevent contamination of room air with the radionuclide. The camera was generally centered posterior to the kidney, and the probe-mounted scintillation detector was located anteriorly. In one normal subject and in two patients with transplanted kidneys, the positions were reversed.

Instrumentation. A scintillation camera (Searle Radiographics Pho/Gamma III) with a 4000-hole low-energy collimator was used. A 25% window was set symmetrically over the ^{133}Xe photopeak (81 keV). The spatial resolution of the detection system was determined for ^{133}Xe at various distances from the collimator with Lucite (tissue-equivalent material) interposed between the line source and the collimator. Full widths at half-maximum values were 1.94 cm at the collimator surface, 2.16 cm at 2.5 cm from the collimator, 2.20 cm at 4.7 cm, 2.42 cm at 7 cm, and 2.86 cm at 11 cm from the collimator.

The camera was interfaced through analog-to-digital converters to a magnetic video recorder which stored the data in a 256 × 256 matrix. This system permitted the study to be viewed and photographed on the standard camera oscilloscope screen or on an attached persistence oscilloscope; regions of interest could be selected for time–activity analysis.

In addition, the camera was interfaced to a machine analysis system (Nuclear Data 50:50) consisting of a small computer and a dual parameter analyzer with a 4K (24-bit word length) memory. Conventional software supplied by the manufacturer was used for analysis. The camera output was divided into a 64 × 64 matrix for data accumulation. Digitized images were displayed on a 3.5 × 3.5-cm oscilloscope and stored on high-speed digital magnetic tape. Data were integrated over the same time intervals for the camera and the probe.

Analysis. In six normal subjects xenon transit was monitored for 40 min after injection. Curves obtained by isolating the activity from the kidney were analyzed as the sum of four exponential functions by curve peeling (*2,10–14*). In the remaining studies xenon transit was monitored for 5 min, and the smoothed 3-min value was used as an approximation of the two slowest components. Probe and camera data were subjected to compartmental analysis on a coded basis with graphic techniques. The initial slope, as an index of mean flow (ml/gm-min) was obtained by unweighted least-squares on a programmed Wang calculator. Mean and component flow rates were calculated from the slopes with the Kety equations using a hematocrit-corrected partition coefficient. Compartmental distribution was calculated from the zero-time intercepts.

Kidney size at various intervals after xenon injection was assessed in two ways. One technique involved measurement of the area of the image obtained with a Polaroid picture taken from the face of the persistence oscilloscope. The second technique utilized an area measurement from data processed by the computer system.

We first attempted to measure cross-sectional diameter from the conventional scintiphotos obtained directly from the standard gamma camera oscilloscope but phantom studies demonstrated that the apparent diameter of the image increased as a function of the total number of counts collected on the film. This method was abandoned because of the difficulty in collecting the same number of counts over the kidney in each picture and because of the nonlinearity of the Polaroid film at low intensities. We found, however, that a relationship between the apparent size of a radioactive source and its real size as a function of count density could be derived using the persistence oscilloscope. In order to determine the quantitative relationships, a kidney phantom 8 × 3.5 cm was employed into which variable quantities of xenon were introduced. In this way a nomogram relating apparent area (as percent of true area) to count density could be constructed (Fig. 4, inset). This nomogram was employed to correct the apparent renal image to its true size.

A second method used the Nuclear Data system to define a cross-sectional profile of kidney activity at various times during washout. The field was di-

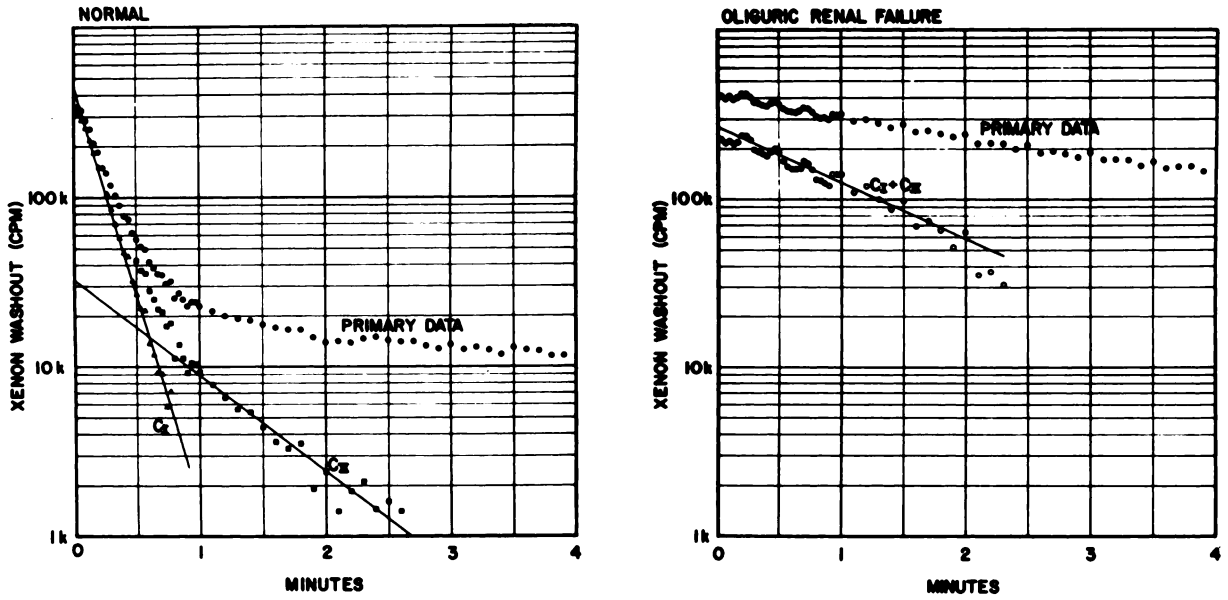

FIG. 1. Examples of time–activity curves obtained with scintillation camera in normal subject (left) and patient with acute oliguric renal failure (right). Washout curves obtained with camera are identical to those obtained with probe-mounted scintillation detector.

vided into a 64 × 64 matrix. The row corresponding to the coronal midportion of the kidney was displayed on the oscilloscope with the count intensity as amplitude along the ordinate and the distance across the kidney along the abscissa. Phantom experiments with a cylinder containing ^{133}Xe suggested that cross-sectional dimension were most accurately measured using the 50% of peak points as the borders. Thus these were used to determine the cross-sectional diameter of the kidney.

To determine kidney area rather than diameter, each element in the 64 × 64 matrix was displayed as an intensified dot on the oscilloscope (Fig. 3). By displaying only elements containing counts greater than 50% of the peak, we were able to measure areas during washout by summating the intensified points, thus avoiding distortion due to film response. The reproducibility of this approach was excellent. Paired, coded determinations by independent observers showed a close correlation in 15 replicate studies ($r = 0.89$, $F = 47.3$; $p < 0.001$).

Mean values have been presented with the standard error of the mean as the index of dispersion. Tests of statistical significance were made with Student's t-test.

RESULTS

Comparison of transit-time measurements by probe and camera. Digital data obtained from the scintillation camera by isolating the activity over the kidney showed characteristics similar to those usually obtained with probe-mounted scintillation detectors in normal subjects and patients (Fig. 1). Group values for mean flow, compartmental flow rates, and compartmental distribution assessed by the probe and the camera in normal subjects and patients with hypertension (Table 1) showed similar results. The only significant difference was the value of residual activity at 3 min, which was greater for probe than for camera studies in both groups. Correlation between the values for compartmental flow rates was excellent ($y = 0.99 \times +3.1$; $r = 0.91$; $p < 0.001$).

Distribution of activity with time. The size of the kidney image fell significantly during the first minute in every normal and hypertensive subject with normal renal function. All had normal rapid flow components of xenon washout (Figs. 1 and 2). Figure 2 represents serial images from the same two subjects whose washout curves are presented in Fig. 1. In the normal subject, a reduction in size was readily apparent at 18–21 sec when only 10% of the initial activity was present in the rapid component. In the patient with acute renal failure, the renal image was unchanged at this time; an unequivocal reduction of renal size was not apparent until 45 sec after injection. A progressive reduction in size of the renal image and the appearance of isotope in the lung by 30 sec were also evident in the computer reconstruction of xenon transit through the normal kidney (Fig. 3).

Some of the apparent decrease in kidney size shown in Fig. 2 is due to the rapid fall in count density. The insert in Fig. 4 shows the relationship between count density and apparent size of a test

TABLE 1. COMPARTMENTAL FLOW RATE AND DISTRIBUTION IN NORMAL AND HYPERTENSIVE PATIENTS

	Component (%)						Flow rates (ml/gm/min)					
	I		II		3 min		I		II		Mean	
	P*	C	P	C	P	C	P	C	P	C	P	C
Normal	78.5	84.1	14.7	12.8	6.8	3.0	4.5	4.4	1.1	1.1	3.6	4.1
(11)	±3.7	±1.7	±2.7	±1.6	±1.2	±0.5	±0.3	±0.3	±0.07	±0.06	±0.3	±0.2
t	1.38		0.60		2.86		0.28		0.35		1.58	
p	0.2		0.6		0.01		0.8		0.8		0.2	
Hypertension	72.9	76.7	20.1	20.0	7.0	3.3	4.9	4.6	1.1	1.2	3.2	3.6
(10)	±7.5	±6.3	±6.4	±5.9	±1.3	±0.5	±0.5	±0.3	±0.05	±0.06	±0.55	±0.3
t	0.38		0.01		2.55		0.49		1.2		0.26	
p	0.8		0.99		0.02		0.4		0.3		0.9	

* P = Probe-derived data; C = data acquired with the scintillation camera.

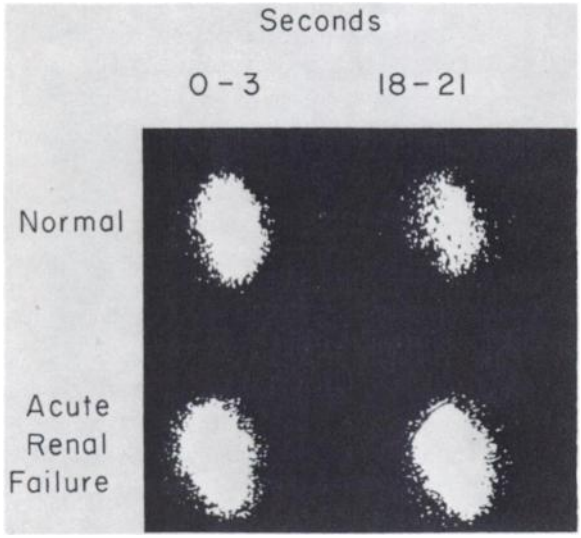

FIG. 2. Serial images from same two subjects whose washout curves are represented in Fig. 1. Note striking reduction in size of normal kidney's image apparent within 21 sec. At this time only 10% of initial activity was still present in rapid component. In patient with acute renal failure size of renal image was unchanged at this time.

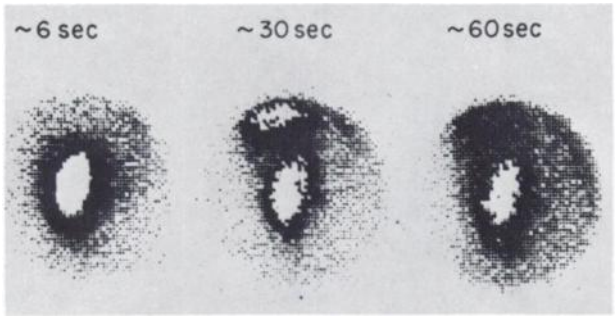

FIG. 3. Xenon transit through normal human kidney defined by computer reconstruction of scintillation camera output. Computer processing avoids effect of count density on appearance of image. Note progressive reduction in size of renal image and appearance of isotope in lung by 30 sec.

object measured on Polaroid film. The relationships between change in area and time corrected for count density in the same two subjects are also shown in Fig. 4. The apparent 50% reduction in renal size in the normal subject's scintiphoto at 18 sec represents a true reduction of about 9%. The more rigorous test also showed that a true reduction in image size (and by inference preferential disappearance of isotope from the renal cortex) did not occur until after 45 sec in the patient with acute renal failure.

The time-related size change derived from the computer reconstructions was in good accord with the above assessment. There was a mean reduction of about 19% in the size of the renal image during the first 40–60 sec of xenon disappearance from the normal human kidney (Table 2). A reduction of this magnitude is consistent with clearing of isotope from the renal cortex prior to its disappearance from more central portions of the kidney. In three oliguric kidneys assessed by this approach, a reduction in size of the renal image did not occur in the first 40–60 sec, in accord with the characteristics of the scintiphotos described before.

Segmental perfusion. The upper and lower halves and upper and lower thirds of the kidneys showed a small difference in the initial slope's half-time from the various regions (Fig. 5). Half of the observations made in the hypertensive populations fell outside the 95% confidence intervals for normal subjects (including four of ten studies in patients with essential hypertension and three of four in patients with chronic pyelonephritis). One of the three patients with renovascular hypertension also showed a gross discrepancy in segmental intrarenal perfusion.

Review of the arteriograms without reference to the flow data revealed, in some cases, a correlation between discrepancies of regional perfusion and

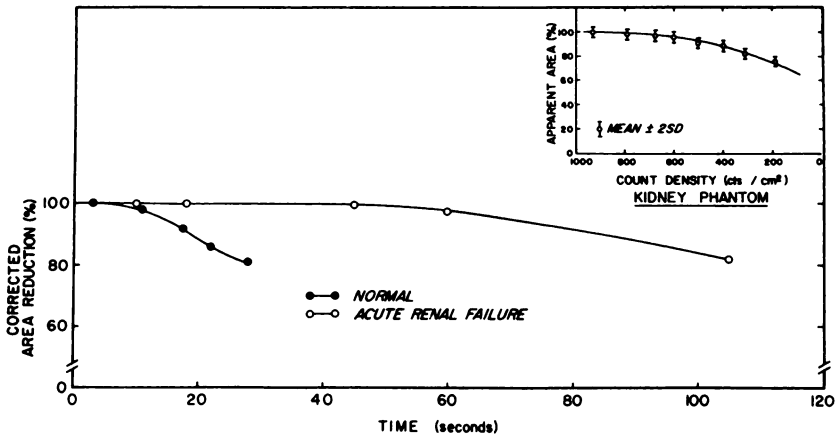

FIG. 4. Insert shows relationship between count density and apparent size of object derived from studies with phantom. Note that for count densities below approx 600 counts/cm², apparent area is reduced. When size of image is corrected for count density, progressive reduction of approx 20% occurs in normal subject within 20 sec.

TABLE 2. CHANGE IN RENAL AREA WITH TIME*

Time (sec)	Reduction (%)
0–10	100
30	86.4 ± 4.7
60	81.0 ± 5.7

* Determined from computerized camera data.

characteristics of the arteriogram. Local changes included localized thinning of the renal cortex with pyelonephritis or nephrosclerosis. In other patients, however, an equivalent discrepancy in segmental perfusion was not associated with demonstrable local differences in the selective arteriogram.

A relationship was apparent between the percentage of flow in the rapid component defined by compartmental analysis and the disparity between the xenon turnover in different segments of the kidney. In the nine patients in whom over 80% of the flow was in the rapid component, the absolute difference in half-time between the upper and lower thirds was 1.9 ± 0.6 sec. In five patients in whom the rapid component represented less than 60% of the total (the lower limit of normal with this method), the absolute difference in half-time was 8.3 ± 2.3 sec ($t = 2.49$; $p < 0.05$). For the eight subjects in whom an intermediate percentage of flow in the rapid component was found, the mean difference was also intermediate (3.4 ± 1.6 sec).

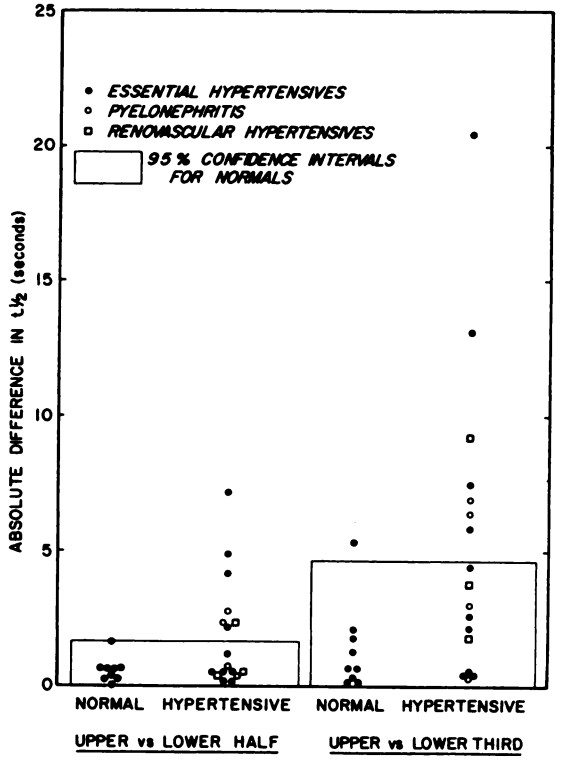

FIG. 5. Segmental renal perfusion in normal and hypertensive patients.

DISCUSSION

Evidence that the early rapid component of xenon washout from the kidney represents cortical perfusion is compelling but not conclusive. Recent studies in man with the scintillation camera seemed to provide a clear and relatively direct confirmation (*17,18*). In these studies a progressive reduction of the size of the renal image with time was compatible with the preferential disappearance of isotope from the outer portions of the kidney (i.e., a more rapid turnover of isotope and thus higher flow rates in the cortex). Our own evaluation of the scintillation camera, however, made it apparent that the size of the image was related not only to the size of the object but also to the level of incident radioactivity. For

this reason it was necessary to apply a more rigorous method.

The two methods were adopted in the study presented here and involved a correction of the scintiphoto for incident radioactivity and a computer-derived reconstruction of the image. Both methods gave the same results. The image did decrease in size during xenon washout from the normal kidney and the magnitude of the reduction was compatible with disappearance of isotope from the renal cortex prior to its disappearance from more central portions of the kidney. The 19% reduction demonstrated during the first minute of xenon disappearance is in striking accord with calculations made from models with dimensions of the human kidney. Thus for a kidney which is 12 cm long, 7 cm wide at its widest, and has an approximately 1-cm rim of cortex, there is a calculated 21% reduction in area on the basis of an en-face prolate spheroid. The two limiting cases (i.e., a rectangle with 7 $\times$ 12 dimensions or a circle with an approximately equivalent area) showed a 20% reduction in the area with the removal of the outer centimeter along the border.

Absence of the rapid component in patients with acute oliguric renal failure, supported by angiographic and morphologic studies, has suggested a preferential diffuse reduction in cortical perfusion (*11*). The present study directly supports this interpretation. In the four patients with acute renal failure, the early progressive decrease in renal size evident in the normal subjects did not occur; rather the reduction in size occurred much more slowly. Thus it appears that cortical flow is present in acute renal failure but is uniformly decreased to about one-third of normal. It is of interest that the variability of blood flow described earlier in patients with acute oliguric glomerulonephritis (*20*) was also seen in the patient whose data are shown in Fig. 1: this patient had an acute vasculitis. Immunologic attack upon the renal vasculature appears to result in vasomotor activation which may well participate in the pathogenesis of the renal failure.

The anatomic distribution and physiologic implications of the slower components of xenon disappearance were not delineated. It was our hope that regional perfusion in more central portions of the kidney could be evaluated with the scintillation camera. Unfortunately, the instrument's efficiency and spatial resolution were insufficient to allow such an analysis. It was apparent, however, that the scintillation probe used in this and most other studies views a region larger than the kidney. The percentage of residual activity seen by the probe 3 min after injection was approximately twice that in the area defined as the kidney by the scintillation camera. The radioactivity outside the kidney probably reflected recirculating radioxenon in the abdominal fat stores. Although the data makes it clear that this factor influences little the values of the first and second components, recirculation must have important implications for the tail components as suggested by Ladefoged (*9*).

The limited spatial resolution and efficiency of the instrument also limited the assessment of segmental intrarenal perfusion. The technique was adequate, however, to allow assessment of the two halves of the kidney, and more rigorously, the upper and lower poles. When smaller volumes of tissue were examined, the limited efficiency resulted in low counting rates and statistical error became critical. For this reason a least-squares solution was used to define the mean flow. This situation should be improved considerably with the newer camera collimators and electronics (*21*) and with the introduction of ^{127}Xe and ^{135}Xe.

We anticipated a quantitatively important difference in regional intrarenal perfusion in patients with chronic pyelonephritis, a disease characterized by a patchy asymmetrical lesion. Such a difference was found. We were surprised to find an equivalent prevalence and degree of flow asymmetry in patients with essential hypertension. The abnormality was associated with a reduction in the size of the rapid flow component as anticipated in the presence of patchy renal microvascular disease (*13*). The findings suggest that nephrosclerosis is not uniformly distributed throughout the kidney but is sufficiently focal that quantitatively important regional differences in perfusion may occur. It is possible that advances in the technical quality of the renal arteriogram and in the spatial resolution and efficiency of the scintillation camera will provide a much more precise evaluation of this phenomenon.

ACKNOWLEDGMENTS

It is a pleasure to acknowledge the help provided in various parts of this study by Michael A. Davis, Kathern J. Hinrichs, Linda Guiod, Sally Edwards, Beverly Mahabir, Pricillia Price, and Lorraine Rodolph. This work was supported in part by NIH Grants GM18674, HL11668, and HL05832 and Army R&D Command contract DA-49-193-MD-2497. The studies were carried out in the Clinical Research Center of the Peter Bent Brigham Hospital, supported by NIH Grant SM01-FR-31-08.

REFERENCES

1. KRAMER K, THURAU K, DEETJEN P: Hämodynamik des Nierenmarks, I. *Pfluegers Arch* 270: 251–269, 1960

2. THORBURN GD, KOPALD HH, HERD JA, et al: Intrarenal distribution of nutrient blood flow determined with krypton^{85} in the unanesthetized dog. *Circ Res* 13: 290–307, 1963

3. AUKLAND K, BOWER BF, BERLINER RW: Measurement of local blood flow with hydrogen gas. *Circ Res* 14: 164–187, 1964

4. WOLGAST M: Studies on the regional renal blood flow with P^{32} labelled red cells and small beta-sensitive semiconductor detectors. *Acta Physiol Scand [Suppl]* 313: 1–109, 1968

5. STEINER SH, KING RD: Nutrient renal blood flow and its distribution in the unanesthetized dog. *J Surg Res* 10: 133–146, 1970

6. MCNAY JL, ABE Y: Pressure-dependent heterogeneity of renal cortical blood flow in dogs. *Circ Res* 27: 571–587, 1970

7. SUKI WN, POLANYI ML, OSTROWSKI D, et al: Measurement of intrarenal transit time and hemoglobin saturation by fiberoptics. *J Appl Physiol* 29: 123–126, 1970

8. SLOTKOFF IM, LOGAN A, JOSE P, et al: Microsphere measurement of intrarenal circulation of the dog. *Circ Res* 28: 158–166, 1971

9. LADEFOGED J: *Renal Circulation in Hypertension.* Copenhagen, Munksgaard, 1968

10. ROSEN SM, HOLLENBERG NK, DEALY JB, et al: Measurement of the distribution of blood flow in the human kidney using the intraarterial injection of ^{133}Xe. Relationship to function in the normal and transplanted kidney. *Clin Sci* 34: 287–302, 1968

11. HOLLENBERG NK, EPSTEIN M, ROSEN SM, et al: Acute oliguric renal failure in man: evidence for preferential renal cortical ischemia. *Medicine* 47: 455–474, 1968

12. HOLLENBERG NK, EPSTEIN M, ROSEN SM, et al: Vascular lesions of the transplanted human kidney—morphologic and hemodynamic studies in chronic rejection. *Trans Assoc Am Physicians* 81: 274–287, 1968

13. HOLLENBERG NK, EPSTEIN M, BASCH RI, et al: "No man's land" of the renal vasculature. An arteriographic and hemodynamic assessment of the interlobar and arcuate arteries in essential and accelerated hypertension. *Am J Med* 47: 845–854, 1969

14. EPSTEIN M, HOLLENBERG NK, MERRILL JP: The pattern of the renal vascular response to epinephrine in man. *Proc Soc Exp Biol Med* 134: 720–724, 1970

15. GRUNFELD JP, KLEINKNECHT D, ASSAILLY J, et al: Intrarenal distribution of blood flow, cardiac output and renin secretion in hypertensive patients. Abst Radionuclides in Nephrol (Int Symposium), sponsored by Int Soc Nephrol, Soc Nucl Med, 1971, p 4

16. DELL RB, SCIACCA R, LIEBERMAN K, et al: A weighted least-squares technique for the analysis of kinetic data and its application to the study of renal ^{133}xenon washout in dogs and man. *Circ Res* 32: 71–84, 1973

17. BLAUFOX MD, FROMOWITZ A, GRUSKIN A, et al: Validation of use of xenon 133 to measure intrarenal distribution of blood flow. *Am J Physiol* 219: 440–444, 1970

18. KEW MC, VARMA RR, WILLIAMS HS, et al: Renal and intrarenal blood-flow in cirrhosis of the liver. *Lancet* 1: 504–510, 1971

19. HOLLENBERG NK, EPSTEIN M, BASCH RI, et al: Renin secretion in the patient with hypertension: relationship to intrarenal blood flow distribution. *Circ Res* 24 (Suppl 1): 113–122, 1969

20. EPSTEIN M, BERK DP, HOLLENBERG NK, et al: Renal failure in the patient with cirrhosis. The role of active vasoconstriction. *Am J Med* 49: 175–185, 1970

21. ZIMMERMAN RE, HOLMAN BL: Modulation transfer function for the Pho/Gamma III and Pho/Gamma HP scintillation cameras using ^{99m}Tc and ^{133}Xe. *J Nucl Med* 13: 481–482, 1972